NAL PROPOSAL No. 256

Scientific Spokesman:

L. Osborne
Laboratory for Nuclear Science
Massachusetts Institute of Technolog
Cambridge, Massachusetts 02139

FTS/Comm: 8-253-1000

2nd GENERATION ELECTRONIC NEUTRINO DETECTOR AT NAL

D. Frisch, D. Luckey and L. Osborne (MIT)
B. Cox (NAL, M. Perl (SLAC)

October 1973

2nd GENERATION ELECTRONIC NEUTRINO DETECTOR AT NAL

D. Frisch, D. Luckey and L. Osborne (spokesman) (MIT);

B. Cox (NAL); M. Perl (SLAC)

Contents:

A. Introduction

We propose the development of a 2nd generation neutrino detector at NAL. This detector, which will require a new building, will be a very large device using counter and electronic track-chamber techniques. The emphasis is on 2nd generation physics, for which the present detectors (New 1a, New 21a, and 15'BC) are not optimal.

In particular, we want a massive target of hydrogen or deuterium in an apparatus designed to identify and measure muons, electrons, photons, and charged hadrons over essentially the entire 4π solid angle. This will enable the study of the form factors of neutrons and protons through deep inelastic neutrino scattering at the largest q^2's available at NAL, with the necessary uniformity of response as a function of the kinematic parameters, and with the necessary unambiguous distinction between neutral and charged current events.

In addition, a major capability of the facility will be to study the details of the final state hadron system. Again, the simple target and the full solid angle in muon acceptance are essential for this work. We anticipate that studies of their multiplicities, and of the correlations between their vector momenta, and of their momentum-charge correlations, will all be of fundamental importance in understanding the underlying structure of the hadrons.

Below is a more detailed account of the physics capability and the present preliminary concept of such a device.

B. Purposes

Table 1 (pp. 6 and 7) gives a pithy summary of the physics especially addressed here. More broadly — see Appendix 1 — some of the forseeable purposes of developing neutrino detection further at NAL are:

1. Studies of the details of hadron formation in deep inelastic neutrino interactions, allowing comparison with hadron formation in electromagnetic and strong interactions. (See Question 5, Table 1.) This will be one of the most powerful tools for study of parton dynamics.

Already the sign-momentum correlations among the hadrons produced in deep inelastic electron scattering (Dakin et al PRL 31 786 (1973)) are being compared with quark model predictions (Kuti and Weisskopf Phys. Rev. D 4, 3418 (1971)). For example, does the emitted pion with the greatest momentum keep the sign of electric charge of that parton which got the initial impulse in the reaction? If so, the average negative to positive charge ratio for leading pions in electron scattering should be 1:8 for "valence" quarks and 1:1 for "core" quarks. But in neutrino interactions this negative to positive ratio should always be zero, because a charged lepton made by a neutrino on ordinary matter must be negative, so the recoil quark must be positive. The possibilities are of course greatly enriched by neutral currents.

Thus correlated sign and momentum measurements of the hadrons - including π^o's and K^o's - produced in deep inelastic neutrino scattering may well prove necessary to the unscrambling of basic parton interactions from the problems of their deexcitation and reclothing to form the observed hadrons.

This work can be done with a broad band beam, provided the detector can measure both the lepton momentum $p_\mu(e,\nu)$ and the hadron energy E_h. Both ν's and $\bar{\nu}$'s are necessary, and both H_2 and D_2 as targets. The expected yields are given in Table 2 (p. 8).

2. Precise studies of the dependence of the differential deep inelastic cross-sections on energy loss $E_\nu - E_\mu$, on four momentum transfer q, and on neutrino energy E_ν. (Questions 1 through 4, Table 1.)

Such experiments are complementary to electron and muon deep inelastic scattering, using weak rather than electromagnetic forces as probes. They should be made at energies $E_\nu \gtrsim 20$ Gev in order to probe the "scaling region" where the proton's rest energy is expected to be negligible. These studies too should be done using both ν's and $\bar{\nu}$'s, and both H_2 and D_2, and in addition using both ν_μ's and ν_e's.

This work should be done with a narrow band beam so as to have a cross-check on the neutrino energy, which is also found as the sum of the observed μ (or e) energy and the hadron energies. One would hope ultimately to use a tagged beam to get the incident neutrino energy even more precisely, and especially in the cases where there is an unmeasureable outgoing neutrino instead of a measureable outgoing μ or e.

To explain that neutral currents apparently exist for $\Delta S = 0$ and not for $\Delta S = 1$ (eq. in K decays), "charmed" particles have been introduced in several models (Weinberg Phys. Rev. D5 1412 (1972); DeRujala and Glashow, Harvard Univ. Lyman Laboratory Preprint (1973) and Physics Letters (to be published)). Such theories invalidate the simple relation

$$F(\nu p) = F(\bar{\nu} n)$$

for both charged and neutral currents, so that it becomes even more imperative that good measurements be made on neutrons and protons separately, and with monochromatic beams of ν's and $\bar{\nu}$'s in separate runs.

Some expected yields using ν_μ's are given in Table 3 (pp. 9 and 10), and it is seen there that a very large and well-understood detector is necessary to probe the very deep inelastic region, especially to look for the effects of W's on high-q^2 propagators. It is clearly very important that there not(!) be biases in acceptance that vary strongly with x and y.

The "elastic" reaction $\nu_\mu + n \rightarrow \mu^- + p$ and the only slightly inelastic reactions such as $\nu_\mu + p \rightarrow \mu^- + \Delta^{++}$ will probably have been studied to some extent in the 15'BC by the time a more advanced electronic detector is built. However, there will be much value in repeating these experiments to get higher statistics and to go to higher energies, especially since the small-q^2 cross-sections can be assumed with confidence to be the same function of q^2 at high energy as at low and can thus be used to find the neutrino spectrum. Such knowledge of the spectrum is necessary to get the E_ν dependence of each cross-section. While the E_ν dependence of the cross-section is not explicitly needed for each of the studies listed in Table 1, it will allow important cross-checks and, if the existence of W's is to be inferred, these must be precision experiments with as many serious cross-checks as possible.

3. Search for new reactions

a. Hadronic products from charged vs neutral currents: As neutrino physics unfolds a lot can happen. For example, perhaps there is a strong correlation between charged vs neutral currents and production of strange vs non-strange particles at high energies. Versatile detectors of great sensitivity such as this one, will amost certainly be extremely important for some of this work.

b. $W^{\pm}$ production: If there is any hint of the observation of real $W^{\pm}$ decays in the first generation experiments it will be urgent to distinguish unambiguously the $W \rightarrow e + \nu$ and $W \rightarrow$ hadron modes and to measure unambiguously the sign of the low energy $\mu^-(e^-)$ accompanying W-production by $\nu_\mu(\nu_e)$.

c. Exotica: To recognize such reactions as $\nu_\mu + p \rightarrow e^+ + n$ will likewise require more versatile and senstitive detectors, since rare events need particularly reliable discrimination against many types of backgrounds. In some reactions great energy precision may be needed and fortunately there is hope that ultimately neutrino tagging can be developed for use with electronic detectors, such as this one.

Table 1:

Physics Questions Answered by Studies of Inelastic Neutrino Scattering $\nu(\bar{\nu}) + p(n) \rightarrow \mu^-(\mu^+) + \text{All}$

Definitions: $\nu \equiv E_\nu - E_{\mu(e,\nu)}$; $q^2 \equiv |p^4_\nu - p^4_{\mu(e,\nu)}|^2$; $x \equiv \frac{q^2}{2M_p\nu}$; $y \equiv \frac{\nu}{E_\nu}$

$$\frac{d^2\sigma^{\nu(\bar{\nu})}}{dxdy} = \frac{G^2ME_\nu}{\pi}\left[(1-y)F_2^{\nu(\bar{\nu})} \pm xy^2F_1^{\nu(\bar{\nu})} \mp xy\left(1-\frac{y}{2}\right)F_3^{\nu(\bar{\nu})}\right]$$

(The F's are "structure functions", functions of q^2 and ν, with scaling saying they are functions of $x = \frac{q^2}{2M\nu}$ only.)

Question	Effect of "Yes" Answer on $\frac{d\sigma^{\pm(o)}}{dq^2}$
1. Are weak forces carried by heavy bosons $W^{\pm(o)}$ of finite mass $M_{W^{\pm(o)}}$?	1. Breakdown of scaling in ν/q^2 because of $W^{\pm(o)}$ propagator $\frac{1}{\left(q^2 + M^2_{W^{\pm(o)}}\right)}$
2. Independent of their mass(es), do $W^{\pm}$s	2.
a. Have spin 1?	a. $\frac{d\sigma^{\pm}}{dq^2}$ has no terms higher than quadratic in $y = \nu/E_\nu$
b. Couple to spin 1/2 particles only?	b. $2xF_1 = F_2$
c. Have charge summetry?	c. $F_{\nu p} = F_{\bar{\nu} n}$ for all structure functions (F's). But see discussion on p. 3)
d. Give a $V-\gamma_5 A$ interaction with $V = A$ at high energies?	d. $F_2 = xF_3$
e. Couple only to λ core-quarks	e. $\Delta S_{\pm} = 1$ transitions will appear only at small x.
f. Couple equally to electrons and muons?	f. $\frac{d\sigma^{\pm}(\nu_e)}{dq^2} = \frac{d\sigma^{\pm}(\nu_\mu)}{dq^2}$

Table 1 (continued)

Question	Effect of "Yes" Answer on $\frac{d\sigma^{\pm(o)}}{dq^2}$
3. Independent of their mass(es), do W^o's	3.
a. Behave as $W^{\pm}$ as in 2a, b, and c ?	a. Same answers as in 2a, b, and c
b. Couple both to quark and electromagnetic charges ?	b. y behaviour will be a general quadratic reflecting the mixture of couplings
c. Require "charmed" partons ?	c. "Charmed" particles ($M_c > M_p$) will be found with long lifetimes.
4. Is there scaling?	4. All structure functions are $F(\nu/q^2)$ independent of y and E_ν.
5. Do partons evident in deep electron inelastic scattering interact in the same way in neutrino scattering?	5. All neutrino F's will be simply related, through the (model-dependent) weak and electromagnetic charges of point partons, to electron F's.
6. Does hadron formation correspond to that in electron-nucleon and in hadron-nucleon interactions?	6. The distributions of hadronic $p_{\parallel}$, $p_{\perp}$ and multiplicity will be nearly the same, but the charge ratios and $\Delta S = \pm 1$ rates will be different and model-dependent. The hadronic charge ratios may reveal the charge nature of the struck parton.

Table 2

Roughly Estimated Useful Events from H_2 Targets for Hadron Sign-Momentum Correlations in Inelastic Scattering of ν_μ's. ($5 \cdot 10^{18}$ protons of 400 Gev; focused broad-band neutrino beam)

E_ν	x	15'BC (with full EMI)	This Detector (with 3m x 3m H_2 cells)
> 20	>.5	3,000	50,000
	>.8	300	5,000
	>.9	30	500
> 40		1,500	25,000
	"	150	2,500
		15	250
> 80		500	8,000
	"	50	800
		5	80
>160		100	1,600
	"	10	160
		1	16

Table 3 Caption

Roughly Estimated Useful Events for Precision Studies of Form Factors in Inelastic Scattering of ν_μ's

Assume an improved dichromatic beam with 5.10^{18} protons on target at 400 Gev, and 1.10^{18} at 1,000 Gev. Divide by about 5 for a $\bar{\nu}_\mu$ beam, or by about 50 for ν_e or $\bar{\nu}_e$ beams. Detector Parameters as in Table 4.

Round brackets indicate data with exceptionally difficult systematic problems. Square brackets indicate data where the signs and momenta of the hadronic products are not measured.

The first entry for each E_ν is the total elastic yield, proportional to $\int \frac{d\sigma(\bar{E}_\nu)}{dq^2} dq^2$, with $\Delta E_\nu/\bar{E}_\nu = .1$. The second is the yield in the inelastic bin (one of 25 bins), proportional to $\frac{d^2\sigma(\bar{E}_\nu)}{dx\,dy} \Delta x \Delta y$, with $\Delta\bar{E}_\nu/\bar{E}_\nu = .1$ and with $\Delta x = \Delta y = .2$, and with $\bar{x} = .4$, and $\bar{y} = .9$. The third is the inelastic, with everything the same, except $\bar{x} = .9$. (Note that while q^2 is dependent on y, the yields for a given E_ν and x are almost independent of y.) The fourth is the total number of inelastics in this $\Delta E_\nu/\bar{E}_\nu = .1$ bin, but with any x or y. The fifth is the grand total summed over the spread of E_ν's within the upper dichromatic peak.

Some explanation of the comparison with other detectors shown here is given in Section D (p. 15).

Table 3 (see caption)

E_p on target (GeV)	$\bar{E}_\nu$ (GeV)	Kinematic Parameters	$(1 + \frac{q^2}{M_W^2})^{-2}$ M_W Gev/c^2 37.5	75	Detector of Expt 21 on of 1a, as approved	15'BC, with EMI and H_2 (1.5 tons) or D_2	15'BC, with EMI and Ne (20 tons)	This detector with: H_2 (6 tons) or D_2 (12 tons)	This detector with: Ne or Hydrocarbon (90 tons)	This detector with: Low-Z plates (90 tons)
400	100	Elastic →	1.00	1.00	([300])	4	30	15	40	160
		$\bar{x}$ =.4; $\bar{y}$=.9 →	.91	.98	([8,000])	(80)	800	400	[6,000]	6,000
		$\bar{x}$=$\bar{y}$=.9 →	.81	.95	([40])	(.4)	4	2	[30]	30
		All in ΔE_ν bin			([24,000])	(240)	2,400	1,200	[18,000]	18,000
		Total in all ΔE_ν bins			([70,000])	(700)	7,000	3,500	[50,000]	50,000
	190	"	1.00	1.00	([100])	1	10	10	30	120
		"	.84	.96	([2,000])	(20)	200	200	[3,000]	3,000
		"	.69	.90	([10])	(.1)	1	1	[15]	15
		All in ΔE_ν bin			([6,000])	(60)	600	600	[9,000]	9,000
		Total in all ΔE_ν bins			([18,000])	(180)	1,800	1,800	[25,000]	25,000
	240	"	1.00	1.00	([12])	.1	1	1	4	15
		"	.80	.95	([300])	(3)	35	35	[450]	450
		"	.63	.88	([2])	(.02)	.2	.2	[3]	3
		All in ΔE_ν bin			([900])	(9)	100	100	[1,400]	1,400
		Total in all ΔE_ν bins			([3,000])	(25)	300	300	[4,000]	4,000
1000	380	"	1.00	1.00	([40])	.5	4	4	12	50
		"	.71	.93	([1,600])	(16)	160	160	[2,200]	2,200
		"	.50	.82	([8])	(.1)	1	1	[12]	12
		All in ΔE_ν bin			([5,000])	(50)	500	500	[6,600]	6,600
		Total in all ΔE_ν bins			([15,000])	(150)	1,500	1,500	[20,000]	20,000

Approximate Number of events expected in various detectors (with $M_W = \infty$)

C. <u>This Proposal</u>

We discuss here an electronic detector, shown very schematically in Figs 1, 2 and 3 (pp. 20 - 22), and with a first guess at parameters given in Table 4 (p. 19).

This detector will have a large mount of target H_2 (or D_2) to give large counting rates. It will have magnetic analysis throughout, giving detailed analysis of the energetic charged particles and of most of the other charged particles and (converted) γ's in each event. And, if necessary, it will have calorimetric addition of the total energy carried out of the visible region by γ's and charged particles. An all-out effort will thus be made to build a detector which has uniform sensitivity as a function of the kinematic parameters x and y over the widest range.

The design of an all-electronic magnetic detector intended to measure primarily the momenta of very energetic μ's and of the leading hadrons is set by the cost as a function of the following parameters:

1) Strength of magnetic field. The higher the field the greater the momentum precision for analysis of charged particles, in linear proportion, and the cost of the magnet goes up roughly linearly with field (more iron, more coil).

2) Ratio of hydrogen thickness to open space along the beam direction. Open space gives less scattering and more path length before a nuclear collision, and hence gives more momentum precision, but gives less target material per unit length, in effect diluting the hydrogen. The cost of the magnet goes up roughly linearly with the total path length, as does the cost of cryogenics and electronics.

3) The-absolute lateral dimensions. These must be large enough for analysis of the μ's to the order of 10%, a reasonable goal for deep inelastic scattering studies even with the best-understood neutrino beams (dichromatic or even tagged).

The quantification of the limitations on precision set by multiple scattering is given in Appendix 2. Some technical design considerations are given in Appendix 3. Some, but not all, of the costs of components are estimated in Appendix 4. Definite design numbers are used throughout <u>as examples only</u>, with detailed optimization to be done later after Monte Carlo studies.

Our tentative major design conclusions are:

1. The long box-like magnet will have superconducting coils, which would give economy and simplicity if the windings were made in very long modules--perhaps even an indivisible unit. But transportation, assembly, and repair favor assembling the magnet from smaller modules, and a short unit (7.5 m) is used here. It is necessary that there be only a small gap between these macro-modules so that there is no appreciable loss in solid angles for those particles that pass between them. For some purposes (e.g. μ-meson scattering) it may be useful to alternate the signs of the field from section to section.

2. Provision will be made in the cryogenic design for substitution of other liquids (e.g. water, neon or liquid hydrocarbon) in the cells, and in all parts of the design for substitution of solid plates (e.g. C, CH_2, Al or Fe) for the liquid cells.

3. About 1/2 meter minimum lateral displacement from the origin of events to the magnet coils should be sufficient for momentum analysis. In addition the lateral distance available should be at least the thickness of a hydrogen cell-plus-detector module in order to allow the μ's at the largest angles to traverse at least three modules for momentum measurement. The track chambers outside the magnet may serve occasionally for additional μ momentum analysis but are primarily just for μ identification by minimum range.

These requirements have set the magnet aperture at approximately 3m x 3m for the hydrogen target dimensions (3/2m x 3/2m) used here, in turn set approximately by the neutrino beam size at high energies. But all dimensions shown here, especially the target dimensions, are very tentative.

4. The track chambers will probably be proportional drift chambers. These can have the requisite low density and can minimize the cost in electronics. Their relatively long sensitive time (compared with other electronic detectors) will not be disadvantageous in these low event rate experiments. Studies must be made of their stability, behavior in magnetic fields, and multi-track resolution before settling this extremely important choice.

5. The most difficult design choices may be about the energy measurements necessary to get the total energy lost by the neutrino. The μ's and energetic charged hadrons will be momentum-measured quite well, and energetic e's (both from ν_e's and from γ's emitted by energetic π^o's) will also be momentum-measured quite well, since they too will go forward through the H_2. (Note that in such a great length of H_2

the γ's will convert well into e^+e^- pairs). But the hadrons and less energetic γ's going off to the sides will be hard to measure.

Very crude estimates encourage us to believe that the setup of Fig 2, with a wide apron of γ-converter and track sensitive detectors, but with no calorimeters or track chambers on the sides (and top and bottom), will be sufficient for better than 10% energy resolution. But, as a fallback position in Fig 3 we show a (fairly thin) quantameter calorimeter for the γ's going to the sides and (not shown) to the top and bottom. This is followed by track chambers to identify particles and to measure roughly the momenta of the hadrons. Finally there is a crude hadrometer calorimeter out nearest the edge of the magnetic field.

Certainly at the far end of the magnet, and possibly at the end of each of large modules probably with holes in their center for the forward jets of high-momentum particles, there should be calorimeter units to sum up the electromagnetic and hadronic energy emerging downstream. Studies will be made to determine how much material can be put in without interfering with μ and leading hadron analysis. Clearly the effective target length for individual hadron momentum analysis would be much shortened by frequent calorimeters interrupting the otherwise low-density path down the magnetic tunnel.

Some energy will be lost by the stopping of very low energy charged hadrons and by the nuclear interactions of the fast hadrons in the hydrogen before a curvature measurement can be made on them. Three 50 cm. slabs of hydrogen, for example, do not present very much material, but still enough so that we will have to study this problem at length before fixing on a final design.

D. Comparison with Present Detectors

The yields estimated for the various reactions are compared in Tables 2 and 3 with similar estimates for the 15'BC with H_2 and Ne fillings, and with the detectors in Expts 21 or 1a as originally designed. Some considerations are:

1. Neutrino beam: A dichromatic beam or a tagged beam should be used for additional definition of the neutrino energies in precision studies, a cross-check that will probably prove of crucial importance if deviations from scaling are indicated. For this reason the yields in Table 3 have been calculated with a factor of 4 loss in intensity of high energy neutrinos from the restricted acceptance aperture of a well-made dichromatic beam.

2. Geometric Disposition of Target Material: Since the highest energy neutrinos--the ones hard to come by in the rapidly falling neutrino spectrum--illuminate only the region near the beam axis, a given amount of H_2 or Ne can be used much more efficiently in an appropriately designed electronic detector than in the 15'BC. For a mean neutrino flight path of 800 meters, for example, perhaps 80% of the 200 Gev neutrinos from fairly well focused K's will lie within a circle of 0.8 meter radius. (This is a very rough estimate pending Monte Carlo studies now being made.) When the accelerator goes up to 1 TeV, so that neutrinos of perhaps 400 Gev will be available in sufficient quantity for useful data, most of them will lie within a radius of only 0.4 meters!

Thus the roughly 40 m^3 of the hydrogen or neon necessary to fill the 15'BC to get a fiducial length of 2 1/2 meters along the beam can be disposed much more appropriately in an electronic detector to give some 15 meters of fiducial length at present accelerator energies, and to give some 60 meters at the anticipated higher energies, with almost proportional gains in yields. We have very tentatively used a fixed 3/2 x 3/2 m^2 cross-section in Table 4, requiring 90 m^3 of cell volume at a target packing fraction of 2/3. It could well be that the best way to take basic data is to fill every other cell with H_2, alternating with D_2, so that even the 15'BC's supplies of H_2 and D_2 would suffice.

3. μ-Momentum measurement solid angle and accuracy: Despite its comparative weakness (5 Kg), the distributed magnetic field of this proposal has two advantages over the lumped field in iron used in the first-generation setups: 1) The μ's from the very deep inelastic scattering at the lower energies stand out at such a wide angle (e.g. E_μ = 2GEV at $\theta \sim .3$ radians for E_ν = 20 Gev and x = y = .9) that a long target with a lumped field misses these μ's unless there are repeated shorter modules, and 2) The scattering of μ's in iron limits the precision of momentum resolution, giving spill-across which will mask the true events, especially in the high energy, high x bins.

4. Hadron momentum analysis: No current electronic detector can analyze individual hadrons at all. The 15'BC filled with H_2 cannot do calorimetry, will miss many μ's even with the EMI, cannot detect π^o's, and has very low rates. The 15'BC filled with neon should be much better in some of these respects, but will give up the clarity of H_2 and D_2 targets necessary to these difficult studies. In addition, it is expected that an electronic detector can cope with a larger muon background, by a factor of at least 10^2, than can a BC, since it can operate with much smaller resolving time and can be given a slow spill. As machine energies

grow progressively higher over the years, the cost and complication of shielding the 15'BC against muons will increase. Thus in the long run the costs of building new electronic detectors may well be compensated for by their lesser demands for shielding and their greater adaptivity for relocation in new beam areas.

5. Hadron energy analysis: Distributed fine grained calorimetry is antithetical to the best μ meson and (especially) hadron momentum analysis--only an $\gtrsim$ 100 m hydrogen bubble chamber can see and analyze everything well without destroying some information. Here the finite cell size, and the necessity for a long low density path for most hadrons, both limit momentum and energy analysis. It is our conviction that a quite comfortable compromise can be made giving $\sim$10% resolution in all important quantities. The price may be a set of expensive scintillation calorimeters forming a long box along the beam, as shown in Fig 2.

6. Yields: For Hadron momentum-charge correlation analysis we have in Table 2 integrated over almost all $(.1<y<.9)$ energy losses, and displayed the integral number of events above various values of x. This is to study the core-vs valence-quark dependence of the data.

For precise form factor studies we have in Table 3 divided the expected inelastic data into 10% width energy intervals in E_ν, and each of these into 5 y-intervals. This is to measure the co-efficients of the expected (general) quadratic in y and also to check that there are no higher terms. Note that the expected y-dependence is not far from flat, so that, crudely, the y-intervals all populated about equally.

We further divide the expected data in Fig 3 into 5 x-intervals to look at the x dependence. Note also the rapid fall off of yields at high x and high y, since $xy \propto q^2$. To the extent that this simple model holds we will measure the structure functions, which we may now compare with those found in inelastic electron scattering.

The deviations most to be sought after are those most simply represented as the effect of a propagator with a single W mass. With a Ne filling in the cells of this electronic detector, there will be some 12 times the number of high energy events at the potentially deviant high end of the spectrum as in the 15'BC filled with the same amount of Ne. The W-mass probed at a given statistical level will thus be almost a factor of two greater. Since we are here just on the borderline of probing the "natural" $M_W = 37.3$ Gev/c^2 region with $E_p = 400$ Gev, this factor of two in W-mass may be critical in exploring the most basic physics and possibly in determining the evolution of high energy accelerators.

However, as the proponents of the Ne-filled BC point out, systematics will be at least as important as statistics in this most important search. While this electronic detector promises higher yields of all events, and more thorough analysis for many types of events, it may be that the Ne BC will give better analysis for some others. We note that a well-designed electronic detector will have a greater flexibility than a BC has for background studies and for changes of target material.

E. Conclusion

A very large electronic magnetic detector is needed at NAL to answer many of the major questions in high energy neutrino physics. It should be feasible using developments of present techniques.

We are making Monte Carlo studies and hope to make electronic detector studies to confirm our strong conviction that the equipment described here will give excellent μ and hadron momentum resolution, and hadron total energy resolution, for these purposes.

Table 4

Summary of Detector Properties

I. Size — Overall 3.7m x 3.7m x 60m
Weight (iron) 2600 tons

II. Magnetic Field (Note: Stored energy is less than half that in 15'BC)
Intensity: about 5 k gauss
Usable Volume: 2.5m wide x 2.75m high x 60m
Disposition: a) In one module or
b) In n modules with the same total volume
Inhomogeneity a) Less than 3%
b) Less than 3% in the module but there will be fringe effects at the ends of each module
Excitation - Superconducting layers of current running parallel to the beam, placed on the vertical sides

III. Target
Composition: Hydrogen and Deuterium (other material can be used if tonnage is desired)
Disposition: Material disposed in 80 cells approximately 0.5m thick. Provision may be made to fill only the cell centers; this makes more efficient use of expensive materials such as deuterium.

IV. Detectors
A. Drift Chambers
Number - 400
Size - 2.5m x 2.5m x 0.025m
Disposition - Sets of 4, measuring x, y, and u, with a fourth to remove right-left ambiguity
Each set is placed between each hydrogen cell, with a set lining the outside of the magnet to measure μ's.
Resolution - 0.5 mm
Track pair resolution - 3 mm (hopefully) - this must await tests

B. Other - Considered but not yet adopted
1. Additional calorimetric measurements along the magnet sides.
2. Cherenkov gas counters between module gaps.

C. Trigger - not required. Information is continually logged in.
Electronic criteria will set the storage condition.

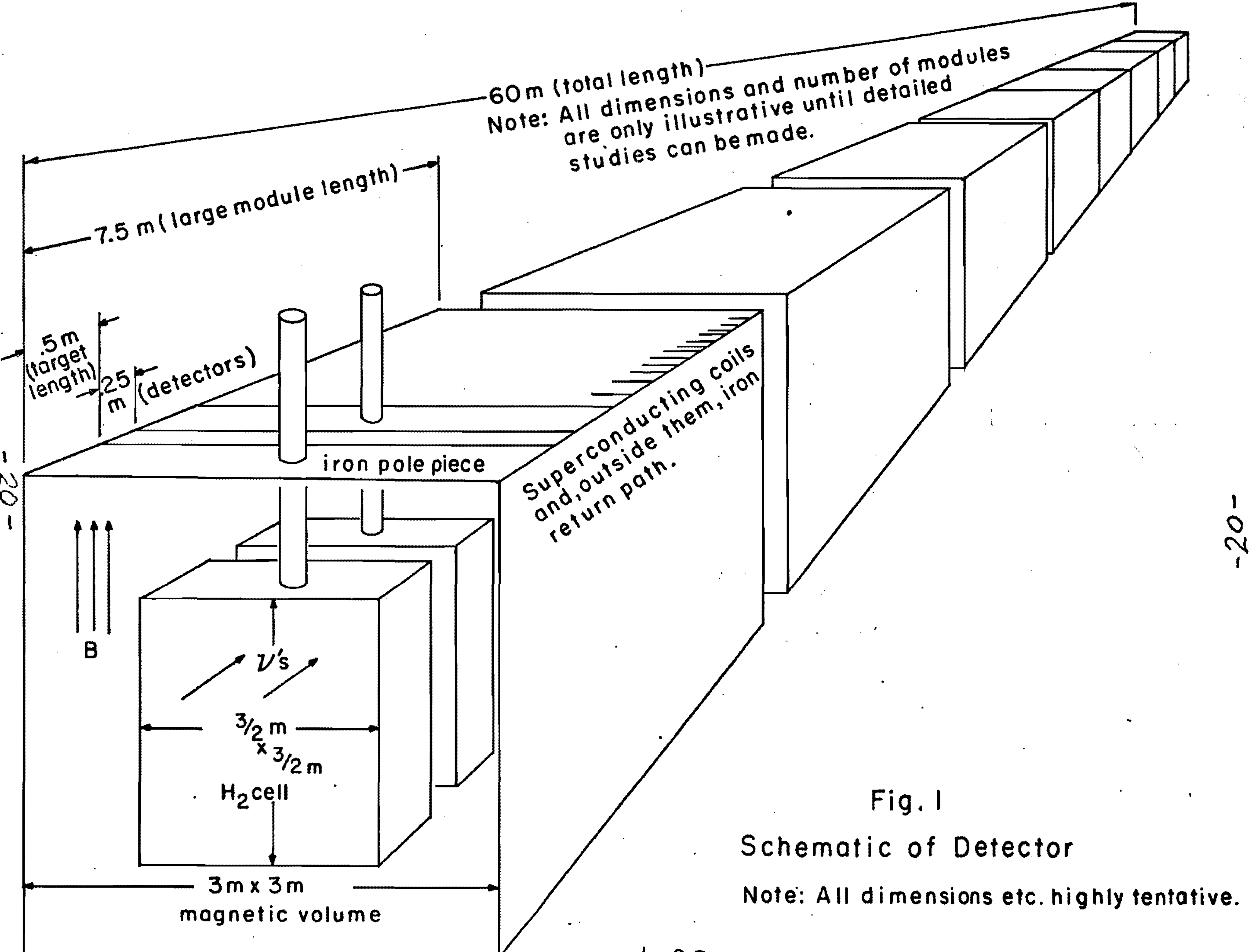

Fig. 1

Schematic of Detector

Note: All dimensions etc. highly tentative.

CROSS-SECTION OF DETECTOR

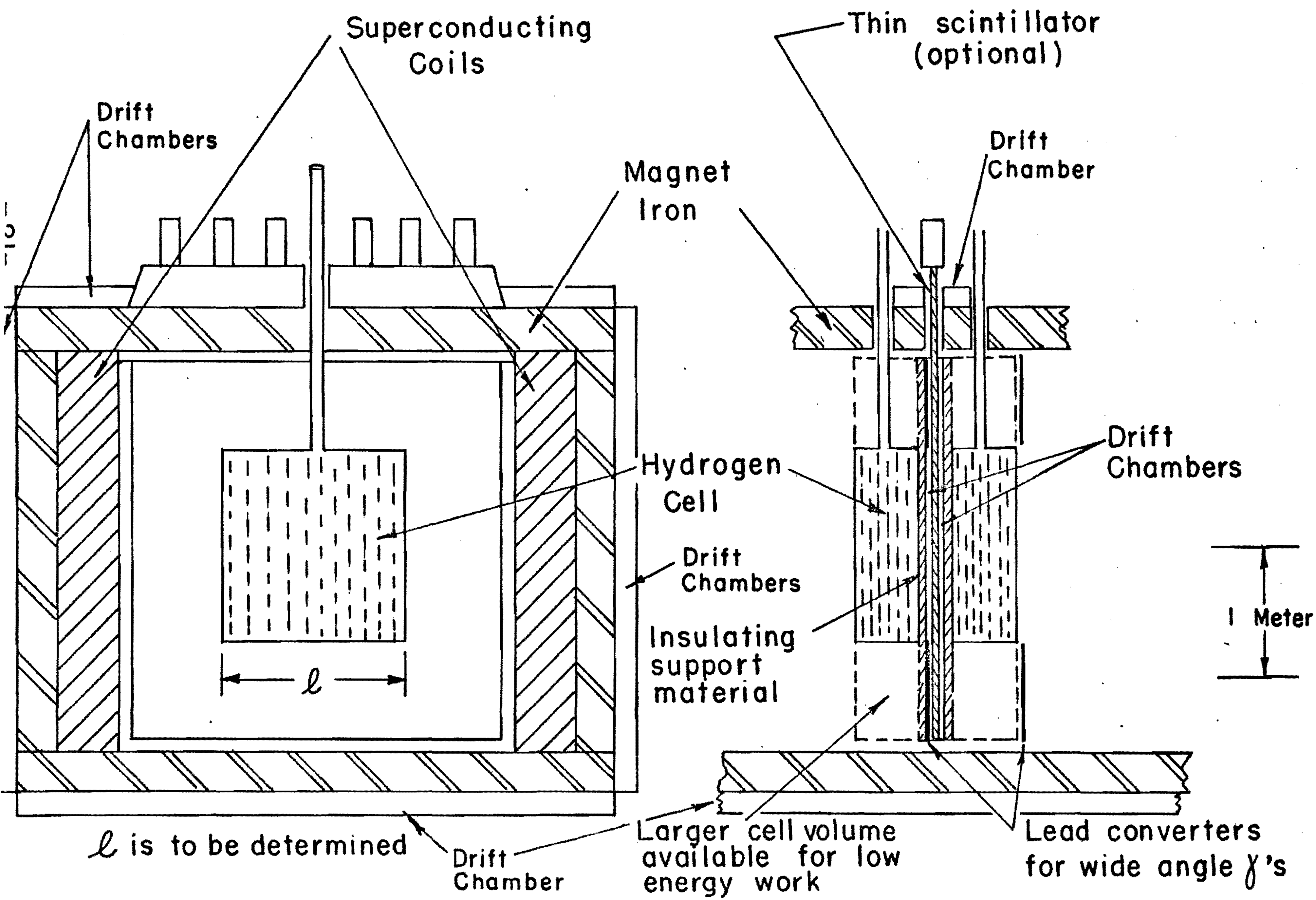

Fig. 2

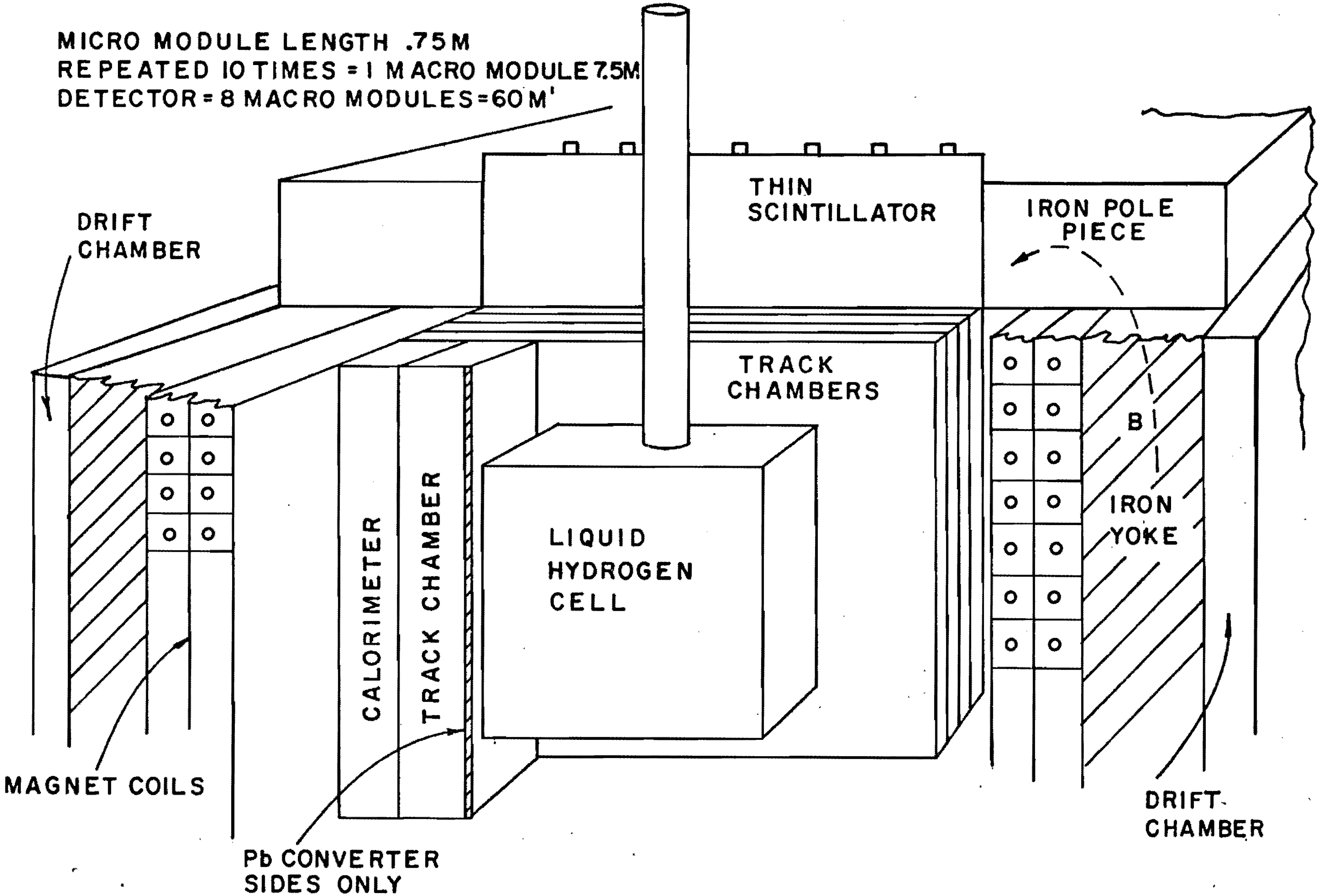

ROUGH LAYOUT: MAGNET AND DETECTORS.

Notes:- 1) RELATIVE DIMENSIONS NOT SET YET
2) TOP & BOTTOM DETECTORS NOT SHOWN

Fig. 3

<u>APPENDIX 1</u>

Some Theoretical Considerations on Neutrino Interactions

The most exciting developments in neutrino reactions up to several months ago were the increasing evidence of agreement of data with the quark model. In particular, the following results (consistent with but not necessarily unique to quarks)

1) $\sigma_\nu = 3\sigma_{\bar{\nu}}$ (See Benvenuti et al PRL <u>30</u> 1084 (1973))

2) $\sigma \propto E_\nu$

3) $\sigma(\nu n) \simeq (1.8 \pm 0.3)\ \sigma(\nu p)$ (G. Myatt and D. H. Perkins PL <u>34B</u> 542 (1971))

This is very poorly measured and emphasizes the need for deuterium as well as hydrogen runs

4) σ_ν flat in y (Barish et al PRL <u>31</u> 565 (1973))

This data can be related to results on deep inelastic electron scattering. The same distribution in $x = Q^2/2M\nu$ seems to be operative in neutrino interactions (Barish et al PRL <u>31</u> 565 (1973)).

In addition studies of the hadronic states in deep inelastic electron scattering (for example Dakin et al PRL <u>31</u> 786 (1973)) have revealed large charge asymmetries in the hadronic final state which may be used not only in the study of the mechanics of hadronic deexcitation but as a diagnostic tool for studying the quark nature of the proton.

More recently there appears to be good evidence for neutral currents (results reported at 1973 Bonn Conf.). This considerably enriches the expected output of any neutrino experiments. It also brings up questions which lay greater stress on the separate measurements on neutrons and protons. Furthermore the analysis of the dynamics requires a knowledge of the neutrino energy. This will require "monochromatic" hadron beams as sources with the inevitable penalty in counting rate. Thus high tonnage targets are even more a desideratum.

The complications of neutral currents can be appreciated by a look at implications for a particular quark model (L. M. Sehgal Preprint, Physikalisches Institut Technische Hochschule Aachen, Aachen W. Germany June 1973). The coupling to proton and neutron quarks is

$$\bar{p}\gamma\ (C_v + \gamma_5 C_A)\ p$$

$$\bar{n}\gamma\ (C_v' + \gamma_r C_A')\ n$$

$$C_A = C_A' = \frac{1}{2}$$

$$C_v = \frac{1}{2}\ (1 - \frac{8}{3} \sin^2\theta)$$

$$C_v' = \frac{1}{2}\ (1 - \frac{4}{4} \sin^2\theta)$$

θ is the Weinberg angle.

In other words the neutral currents couple to both the weak and electromagnetic charge of the quarks. The net result (if all this has any truth) is that the y - dependence of the cross-sections for neutral currents will be more complicated dependence (though still quadratic). Again the neutron-proton separation must be done very carefully and cleanly. The beautiful by product is that we have, in a sense, a way of measuring the quark charges as a reward for the complication.

It is of some interest to note that the Gargamelle results are consistent with the predictions of the above quark model (L. M. Sehgal Preprint Physikalisches Institut Technische Hochschule Aachen, Aachen W. Germany June 1973), namely, the prediction for R and $\overline{R}$

$$R = \sigma(\nu\nu)/\sigma(\nu\mu^-) \simeq 0.2$$

$$\overline{R} = \sigma(\overline{\nu}\overline{\nu})/\sigma(\overline{\nu}\mu^+) \simeq 0.4$$

are consistent.

The problem of neutral currents still remains the elimination of $\Delta S = 1$ neutral currents to explain the small $K \to \mu^+\mu^-$ decay. Various schemes have been suggested.
One of the consequences is that the isotopic spin symmetry

$$F_{\nu p}(x) = F_{\overline{\nu}n}(x)$$

is broken. This reflected not only in neutral current interactions but also in the $\mu^{\pm}$ events. In addition schemes have been proposed introducing "charmed" quarks and therefore "charmed particles. The usual explanation for the lack of observation of such particles is their high mass. Any future apparatus should be able to detect such beasts. This requires magnetic analysis and enough counting rate for high energy interactions.

APPENDIX 2

Measuring Problems

A. Multiple Scattering

With a simple three point measurement with a length L the sagatti δ is given by

$$\delta = X_2 - \frac{1}{2}(X_1 + X_3)$$

and the error by

$$d\delta^2 = dX_2{}^2 + \frac{1}{4}dX_1{}^2 + \frac{1}{4}dX_2{}^2$$

If we take a measuring error $\Delta = .05$ cm and express B in kilogauss, P in GeV/c then one can express the fractional momentum error

$$\frac{\Delta P}{P} = (1.16 \times 10^{-2}) \frac{P}{B\alpha^2}\left[1 + 64\frac{\alpha^2}{P^2}\right]^{1/2}$$

where α is the length L/Length of hydrogen. We have assumed the scattering to be dominated by scattering in hydrogen and have one collision length (374 cm) as an upper limit to the amount of material between measurements.

At this stage since the magnetic field's purpose is to measure the total energy in the hadronic state and to give us an idea of hadron distributions in the hadronic system we put no large premium on a precise Δp measurement. At $p = 50$ Gev, $B = 5$ kg and $\alpha = 1$ we get

$\Delta p/p = 10\%$, which should be good enough.

We may be able to pick out special events such as "elastic" scattering

$$\bar{\nu} + p \rightarrow n + \mu^{+}$$

by coplanarity tests. The neutron would give a nuclear splash downstream of the event point.

B. Detection and Measuring Efficiency

The chief debit of our proposed system is the lack of granularity. As a consequence we may miss low energy secondaries making such a large angle that they miss the detector downstream of the event. The danger here is that either in triggering efficiency or in reconstruction we may bias the x, y, and E_ν distributions. A proper study requires a Monte-Carlo program onto which we have embarked.

In the meantime we can get a rough idea by assuming that the hadronic system has a particle distribution similar to that in hadron collisions.

$$dN \propto \frac{dp'_\ell}{\varepsilon} \quad dp_\perp^{2} \quad e^{-6p_\perp^{2}}$$

Strictly speaking p_ℓ and $p_\perp$ are taken with respect to the frame of the hadronic system.

We estimate our losses by finding the fraction of particles whose p_ℓ is small enough that

$$\frac{\overline{p_\perp}}{p_\ell} > \theta \max = \frac{1}{2} \text{ (say)}.$$

$$\text{Inefficiency} = \frac{\int_0^{p_\ell = 2\overline{p_\perp}} dN}{\int_0^{p_\ell \max} dN} \simeq \frac{2\overline{p_\perp}}{\nu} = \frac{2\overline{p_\perp}}{yE_\nu}$$

We take the distribution in y as flat but cutoff at $y = .05$

$$\text{Inefficiency} \simeq \frac{1.5}{E_\nu} \qquad \overline{p_\perp} = .250 \text{ Gev/c}$$

Rough inefficiency

E_ν (Gev)	Inefficiency %
10	15
20	7.5
40	3.75
80	1.82

The particles we miss, being of low energy, have less leverage in contributing to an error in E_ν.

We also have in inefficiency due to the hadronic system momentum going off at an angle, θ_h

$$\tan \theta_h = \frac{2M\bar{X}}{\sqrt{q^2}} = \sqrt{\frac{2M\bar{X}}{E_\nu y}}$$

Let's apply the same criterion, we "lose" events when $\theta_h > \frac{1}{2}$.

$$y_{min} = \text{Inefficiency} = \frac{4M}{E_\nu}$$

We took $\bar{X} = \frac{1}{2}$ which is not true $(\bar{X} > \frac{1}{2})$ but it is an effective $\bar{X}$ for an unbiased sample in X.

E_ν	Inefficiency (%)
10	25
20	12.5
40	6.25
80	3.12

Note again such inefficiency is y and x dependent.

A2-4

C. Track Separation

1. Properties of Drift Chambers

A particularly difficult problem at high energies is the separation of tracks in the forward "jet". The question is, what is the spread in arrival time of the ionization cloud and what is a practical recovery time for the electronics so that we can distinguish two proximate tracks? We can only estimate these effects at this time; a definitive answer to these questions must await the testing of prototype chambers. The effects which produce this spread are:

a) The lateral diffusion of the electron cloud during the drift time.

b) The inclination of the track with respect to the electric field.

c) The inhomogeneity of the electric field which in turn gives rise to different drift distances for various parts of the track.

d) The recovery time and sensitivity of the electronics. These effects bear on track position accuracy as well.

Present best answers are as follows:

a) The diffusion coefficient for electrons, D, is 259 cm^2/sec.

$$\sqrt{\bar{x}^2} = \sqrt{2Dt} = 0.4 \text{ mm for } 3\ \mu\text{secs.}$$

b) We need only consider the high energy particles for this effect. Their maximum inclination occurs to a great extent because of the angle the hadron jet makes with respect to the neutrino direction. If we have a sensitive depth of 2 cm and an angle of 15° we get 4mm. Monte Carlo studies will be required to find how difficult this problem will be.

c) A good electric guide field can always be made but usually at the price of greater chamber cost. We expect to make measurements on a prototype to see how this variable effects pulse pair separation. We have some guide from our experience in proportional chambers. We are able to retrigger in 100 nsecs and believe this could be lowered to 60 nsecs which represents a space separation of 1.5 mm. This depends to a large extent on amplifier sensitivity (point d).

d) Clock times (>20 mcps) for 50 nsec. accuracy are quite feasible. There remains the problem of a practical amplifier sensitivity; any improvement here will be reflected in track accuracy and pair separation.

We believe it is imperative for prototype work to be started as soon as possible to determine how well we might do in pair resolution.

2. Effects of pair resolution

We calculate below an approximation to event confusion due to pair superposition in a jet. It is natural to take a distribution in rapidity,

$$y = \frac{1}{2}\log\frac{\varepsilon + p_{\parallel}}{\varepsilon - p_{\parallel}} \simeq \frac{1}{2}\log\frac{4}{\theta^2} \qquad \theta << 1$$

We assume a model which fits hadron-hadron collisions to a Gaussian distribution in y and a multiplicity which is the same function of center-of-mass energy. Then

$$dn/dy = 1.59\, e^{-b^2(y_o-y)^2}$$

$$b^{-1} = .59 \log s/3$$

$$s = 2ME\nu\, y(1 - x)$$

$$y = \nu/E\nu \qquad x = Q^2/2M\nu$$

$$\cosh y_o \text{ (c of m rapidity)} = \left[\frac{E\nu}{2m}\ \frac{y}{1-x}\right]^{1/2}$$

We calculate the average multiplicity of particles falling into a cone with $\theta = 1.5 \times 10^{-3}$; this is a cone of 3 mm radius at 2 meters. From this we calculate the probability that 2 or more particles fall into the cone assuming a Poisson distribution

$E\nu$(Gev)	$\bar{n}$ into cone	$P(\geq 2)$
50	1.1×10^{-3}	$.6 \times 10^{-6}$
100	3.4×10^{-2}	5.6×10^{-4}
200	2.26×10^{-1}	.035
400	.63	.13

All this appears to give reasonable tractability; however it is based on our hopes and estimates that a 3 mm separation is possible. We have a further difficulty in that the probability that we obtain overlap in one dimension (in one chamber) is higher.

The spreading due to the magnetic field is, of course, a help. We get

$$\Delta x = 30 \left(\frac{p_1 - p_2}{p_1 p_2}\right) \text{ mm at 2 meters (p's are in Gev/c)}$$

All these problems require the building and testing of a chamber as well as a Monte-Carlo program.

APPENDIX 3

Design Considerations

A. General

We have tried to design a magnetic detector to accommodate a large target volume. The ability to make such an apparently large magnet at a reasonable price is based on the utilization of readily available rolled steel in thick slabs and the avoidance of machining. The use of superconducting coils is chosen to conform with a general policy of minimizing power consumption. The second economy is achieved by the use of the new technique of drift chambers. These allow large spatial coverage at a reasonable cost in electronics.

We have also achieved a certain simplicity in design which should reflect in lower engineering costs. Target and μ-detector are all in one. This gives a high solid angle coverage and the technically easier job of mass-producing identical modules.

We have kept in mind that the final design may call for division of the detector into modules. We lose simplicity of design and use more useless super conductor in back legs, however, the following gains should be kept in mind:

a) Quarter size modules allow manufacture off site with attendant economies

b) Modules allow alternating magnetic polarization which is useful if the detector is used with a μ-beam. See Appendix 5.

c) Other detectors such as Cerenkov counters or additional calorimeters could be inserted between modules.

d) The total mechanical shrinkage of the superconducting coil (1.5" instead of 6") is more manageable.

B. Magnet Iron

1. General Specifications

We have selected a standard steel thickness for the basic slabs, 14". This can be cut and flattened to tolerances of about 1/4". This will be adequate for magnetic tolerances and for simple joining. Sizing is all done by torch cuts. Lower grade steels than magnetic quality might be used; the problem is to check difficulties that might arise from the wider hysteresis loop which might give magnetic field inhomogeneities.

2. Stress Problems

The field which we have picked (5 k gauss) is readily tractable; it corresponds to a pressure of about 30 p.s.i. The top and bottom slabs will deflect 1/8" which is certainly allowable. We plan to take the outward coil stress onto the magnet vertical sides. This does not represent a large stress on our box; it is 23 tons/foot. Such a force can be taken by large bolts.

3. Top Plate

Safety and accessibility will probably dictate that the top plate will be formed of multiple plates and access gaps in between. These gaps need not be large ($\sim$1 foot or less). The magnetic homogeneities will only extend into the magnet to this depth. This region is probably unusable since it would be reserved for cryogenic plumbing, emergency venting, and detector cabling.

C. Magnet Coil

We have given little thought to conventional powering in keeping with laboratory policy of minimizing power usage. Such back of the envelope estimates that have been done do not indicate that conventional power is clearly more economic in just dollar terms. Cryogenic aluminum coils have been considered but seem to be a more costly alternative.

The relatively low field, 5 k gauss, gives only modest thermal losses through structural supports. This loss has been estimated between 150 watts (Purcell) and 400 watts (Mag. Eng. Assoc.). The lower field also reduces the requirements on the super conductor since it will be operating farther from its critical field.

D. Hydrogen Cells

As conceived now the cells are simple rectangular vacuum boxes. A solution to the vacuum forces might be achieved by the use of a honeycomb made from glass based epoxy. It can be tailored to the desired compressive forces, can have holes in the webbs for evacuation, and can have radiator material inserted into the holes. The material is made by Hexcel Corp. All front and back walls could be of 5 mil stainless steel or less; the steel will then have less radiation lengths than the hydrogen (.028 compared to .06).

We have not done detailed designs of these cells.

E. Drift Chambers

We have primarily dwelt on the use of drift chambers over spark chambers for the following reasons:

a) Spatial precision is potentially higher

b) Track pair resolution is potentially higher

c) Operation in a magnetic field is more straightforward.

d) Continuous sensitivity gives lower dead times

e) Sparks and hydrogen are uncomfortable if only psychologically.

The debits of drift chambers rest on the unknowns of a new technique. Some of the detailed problems are brought out in Appendix 2.

The possible use of additional detectors to add conventional calorimetry awaits the development of a Monte Carlo program. Additional detectors such as Cerenkov counters for π-K separation has been only lightly considered. We are confident that our large volume can certainly accommodate such additions were they to prove desirable.

APPENDIX 4

Cost

A. Steel: The fanciest thing to do is use a magnet steel (e.g. Lukens HP); it is also the costliest thing to do. However we have made estimates based on HP (fancy) as well as ordinary low carbon steel (plain).

	Cost/100 lbs. (fancy)	(plain)	Items in $\$10^6$
Base price	8.50	8.50	
Annealing	2.25		
Vacuum furnace	1.75		
Quality control	.60	.60	
Non-optimum dimension	1.50	1.50	
Flatness control	.50	.50	
Edge tolerance	.25	.25	
Total	15.35	11.35	
Total cost of iron (f.o.b. Penn.)	$750,000	550,000	
Assembly	100,000	100,000	
Total	850,000	650,000	.85

B. Magnet Coil

We have two estimates

1. From John Purcell at ANL

a)	Conductor ($0.5/k amp ft)	.30
b)	Cryostat ($5/lb, fabricated)	.84
c)	Insulation	.20
d)	Liquifier	.20
e)	Winding and Assembly	.20
	Total	1.74

B. Magnet Coil

2. From Magnetic Engineering Associates, Cambridge Mass.

(based on 4, 15 meter modules)

a)	Superconductor	.1
b)	Cryostat Modules	.2
c)	Coil Winding and Assembly	.08
d)	Cryogenic plumbing	.06
e)	On site assembly	.1
f)	Power supply	.05
g)	Engineering design and supervision	.15
h)	Liquifier (from B1)	.2
		.94

The second is a more detailed estimate but realism and conservatism dictate weighting the higher price. We take $\$1.5 \times 10^6$

	Total		1.5
C.	Hydrogen Cells		
	a) Fabricated Stainless Steel tanks ($5/lb)	.5	
	b) Hexcel insulation	.1	
	c) Plumbing	.1	
	d) Refrigerator	.2	
	Total	.9	.9
D.	Drift Chambers (based on Harvard chambers)		.75
E.	Drift Chamber Electronics ($20/wire)		.25
F.	Computer Interface and Computer		.15

G.	<u>Building</u>	
	Estimated with the help of T. Toohig (NAL) and based on higher costs considering safety and crane($55/sq. ft.)	.44
H.	<u>Cryogenic Storage and Safety</u>	.25
Grand Total		5.33

APPENDIX 5

Use of Facility for Deep Inelastic μ-Scattering

An intriguing possibility is presented by the use of this facility as a detector of deep inelastic μ-scattering events. Most theoretical models will make a comparison of the structure functions for virtual photon versus neutrino induced reactions. This facility might provide a means of measuring both in the same apparatus, which has the convenience of reducing systematic errors.

The large amount of target material will increase the absolute event rates of particular interest, namely those with large q^2 and ν ($\nu = E_\mu$ (in) $- E_\mu$ (out)). The problem then is to separate out the much larger number of low q^2 events. The latter may be estimated by using the Weizsacker-Williams method combined with the presently measured total photo-production cross-section,

$$\frac{\text{High } q^2}{\text{Low } q^2} \simeq 4\pi^2\,\overline{\nu W_2}\;\frac{m_\pi^{\,2}}{q^2}\;\frac{\log E_\mu/\nu m}{\log^2 E_\mu/m_\pi}$$

q_m and ν_m are the arbitrary lower limits on q dnd ν at which one decides that the events are "interesting". The photon total cross-section has been written as $\alpha\, m_\pi^{-2}$, which is roughly correct.

The technical problem is to avoid all these extra events. The recognition of the large q^2 events is made by "triggering" on μ's that have scattered up and down out of the magnet bending plane since in this direction only events with large $q^2 = 4\,E_\mu(E_\mu - \nu)\,\sin^2\theta/2$ will get out to the periphery of the magnet.

Also, one could not tolerate a large number of low q^2 events, with multi-hadron products, appearing simultaneously with a high q^2 event. In this case one would work with a time spread beam. If the drift chamber is sensitive for 10 μsecs one would limit the beam to get 1 low q^2 event/10 μsecs.

As an example we take q_m = 10 Gev/c

ν_{min} = 10 Gev/c, and High q^2/Low q^2 = 1/5000.

With a beam spill of 1/10 second this implies 20 high q^2 events/pulse. This in turn would require a beam intensity of 3×10^4 μ's/pulse, which should be available with the beam intensity used in Table 2.

The μ-detection may argue for separating the detector magnet into modules; each module could operate with its own polarity. By reversing the field in successive modules the μ-beam passing through the detector can then remain roughly centered.

Appendix 6

Use of 60 Meter Magnet With Iron Target to Search for W Effects in Propagator in Deep Inelastic Scattering, and for Other Reactio

Purposes: We have emphasized in the text the necessity of using hydrogen and deuterium targets to untangle the details of the x and y dependences of the various neutrino cross-sections. In the limit of very high q's, a deviation of the weak interaction propagator from pointlike should appear.

As displayed in Table 3 and indicated in the text, an exceptionally large detector will be necessary to probe W masses if $M_W > 37$ Gev/c^2. For this it will probably be necessary even with $E_p = 1$ TeV to use complex nuclei to get the densest target in kg/m^2. It will of course be risky - and very challenging for theoretical interpretation - to extrapolate from the H_2 and D_2 results with lower q's and E_ν's to results at the higher q's and E_ν's using complex nuclei. Even so, the limits on accelerator energies and intensities expected, and the bigness of the M_W's of greatest current interest, will require an all-out effort with the most massive targets practical.

Many other purposes, some of which are listed in p. 4 and 5, will also be served by making the most dense detector practical, provided that sufficient clarity of interpretation is maintained.

Proposal: We propose here the use of the 60 meter magnet and much of the electronics discussed above, but with iron instead of H_2 as target material and with some new electronic developments. We believe this detector will give data of the greatest reliability and clarity practically attainable in the M_W region of interest.

Fig. A6-1 is a sketch of the 60 meter magnet filled with close-packed iron plates, and with proportional wire planes to serve both as a hodoscope and as an ionization calorimeter. Tentative parameters and cost estimates are given in Table A6-1.

Geometry and Yields: For the highest energy neutrinos, those causing the events with very high q, and for the expected beam geometry at NAL, the irradiated region will be much closer along the axis of the system than our 2.5m x 2.75m target area would indicate. Nevertheless the edges of this area are necessary for good calorimetry, providing room for hadron shower development, even though only the center is irradiated by the highest energy neutrinos.

The irradiated region presents about 100 times as much target as the 15' BC filled with neon. We must multiply the figures in the right hand column of Table 3 by about seven to get the expected yields using 2" iron plates with 1" gaps, i.e. with an average packing fraction of about 0.7. Thus we hope at the highest energies to have some 10^2 events in the highest q bin, and some 10^4 in a typical one of the score of other more typical bins. This should allow measurement of the propagator as e.g. .50 ± .07 for $M_W = 37$ Gev/c^2 or as .80 ± .10 for $M_W = 75$ Gev/c^2, using the intensities put into Table 3.

Hadron Detection: The iron plates shown are thin enough to give good hadron calorimetry, since 2" is about 1/3 of an interaction length.

These plates are also thin enough, and the hadron showers of greatest interest ($E_h \gtrsim 50$ Gev) develop into enough particles, that the angle of the original excited hadron in the elementary interaction will be defined by the lateral ionization density distribution in the hadron shower as it develops to about ± 10%. That is, while it is impossible to determine the original hadron's vector momentum and mass from momentum analysis of the hundreds of final hadrons in this dense medium, it is possible to measure both its total energy and direction, to what (luckily) happens to be about the accuracy we need.

Since we know the incident neutrino direction well from the neutrino beam geometry, the incident neutrino energy can in general be determined to $\sim \pm 10\%$ from the original hadron energy and angle if only two other quantities are measured to comparable accuracy or inferred. Fig. A6-2 displays the knowns and unknowns in reconstructing events with, variously, μ's, e's and ν's emerging.

Monte Carlo studies using models of the hadronic showers are in progress to give a more precise measure of reconstruction accuracy, but it is clear already from these rough estimates that measurement of the direction of the hadronic shower will give valuable cross-checks on μ-out event and e-out event reconstruction in the crucial high-q, rare-event region, and will allow a fit to ν-out events even in a broad-band beam.

Electron Detection: The iron plates are not thin enough to distinguish by shower structure whether electrons are produced indirectly through $\pi^o \rightarrow 2\gamma$, or are produced directly in weak interactions, except when a well developed hadron shower and an energetic electromagnetic shower lie opposite each other about the beam line. Thinner H_2 cells, or perhaps for some purposes very thin aluminum plates, will be necessary for any work with directly produced electrons that cannot be done with the $\sim$0.5m H_2 cells in the main text, e.g. for direct neutrino-electron interaction studies.

Muon Analysis: μ's can be momentum-analyzed in these plates to the desired r.m.s. accuracy of about ±10% at E_μ = 5 Gev and above, with the uncertainty increasing to about ±25% as E_μ goes down to 1 Gev. The range analysis of μ's is good down to about 2 GeV, and lower if the topology of the event allows, so that a μ going out opposite to a well-developed shower about the beam line can be identified and measured even below 1 GeV. The solid angle for μ-detection is the full 4π, a great advantage over other detectors, which rely on μ's emerging after considerable range into a geometrically restricted analysis region.

New Technology: Multi-wire proportional chambers are proposed here both for hadron (and electron) calorimetry and for the μ hodoscope. They will give maximum information about the event, minimize cost and complexity, and allow the highest packing density of iron. Two new techniques contribute to their economical capabilities for these purposes. One is the successful development by Charpak of track localization to about 1 mm even with a spacing of about 10 mm between sense wires, by use of pickup planes measuring the location of tracks along the wire. The other is the promised very rapid development of charged coupled devices, which almost certainly will reduce the pulse height storage cost per wire down to the $1/wire level in a couple of years.

Thus every other plane could consist of sense wires 10 mm apart in one direction, giving ionization location perpendicular to that direction, and also giving total ionization. Alternate planes would have sense wires at 90°. Since hadron showers and, even more, μ meson tracks, extend over many planes, there would be little loss of information. This array would then include only 2.10^5 wires, with readout on 2.10^5 pickup strips.

Table A6-1: Summary of Detector Properties When Used With Iron Plates

(Roughly estimated costs include labor)

I. Size: Overall Dimensions: 3.7m x 3.7m x 60m

Additional Weight Only 2,300 additional tons. Cost approx. $700,000

Total Weight 5,900 tons

II. Magnetic Field (Stored Energy roughly that in 15' BC):

(We thank Dr. Stan Kowalski for making the calculations of field distribution for us, both here and for Table 4 above.)

Intensity: About 12 k Gauss average along path with excitation as in Table 4.

Usable Volume: As in Table 4 (2.5m wide x 2.75 high x 60m)

Inhomogeneity: ∿30% across useful volume. Large fringing field outside magnet.

III. Target:

Composition: Mainly magnet iron

Disposition: Iron plates 2" thick, separated by 1" gaps. Every 30" a wider (2 1/2") gap for drift chambers.

IV. Detectors:

Each gap contains one plane of proportional counter wires serving both as hodoscope and calorimeter.

780 @ 2.5m x 2.75m Proportional wire planes @ $750 mechanics

@ $450 electronics

780 @ 1200 ≅ $940,000

Some scintillators, not shown, should be spaced out through the array to provide a fast μ pulse to be used on occasion in conjunction with a calorimeter time and/or height trigger. It may also be advisable to space out a few very fine-grained proportional wire chambers to be sure that the μ trajectory is clearly defined in the presence of occasional background ionization.

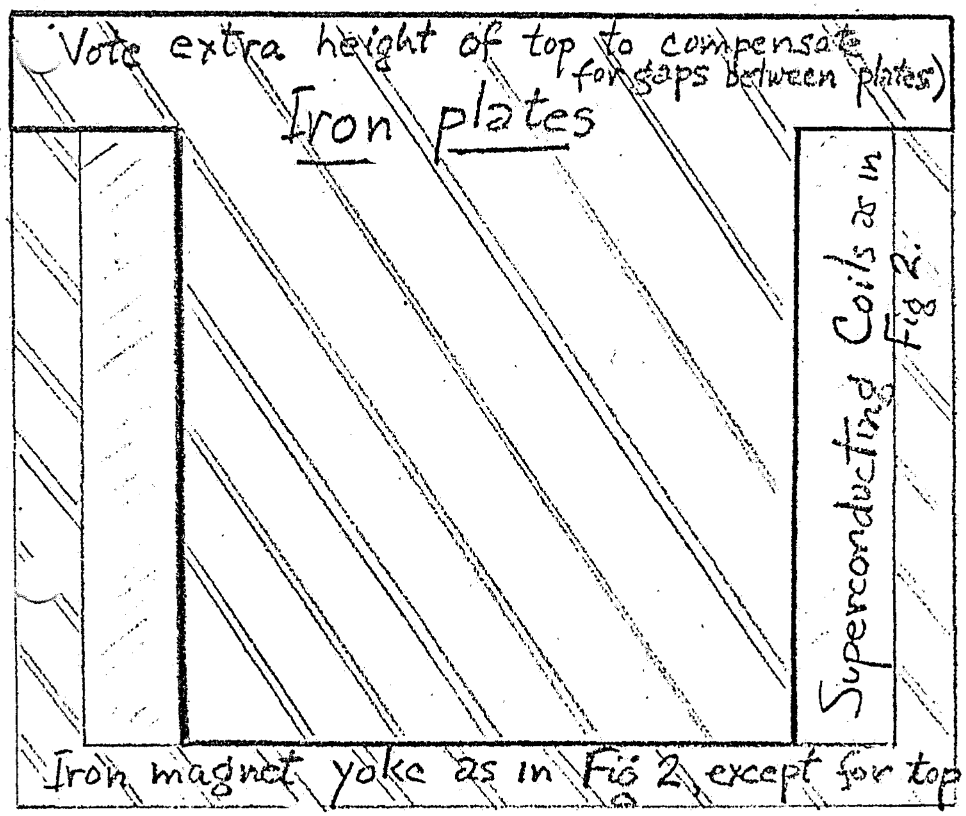

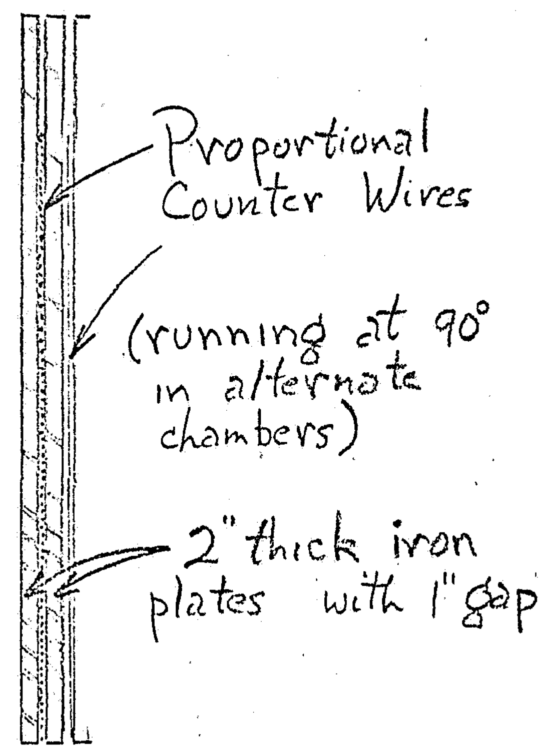

Fig A6-1 Schematic of Magnet with Iron Target

Fig A6-2

EVENT RECONSTR
-ION KINEMATIC

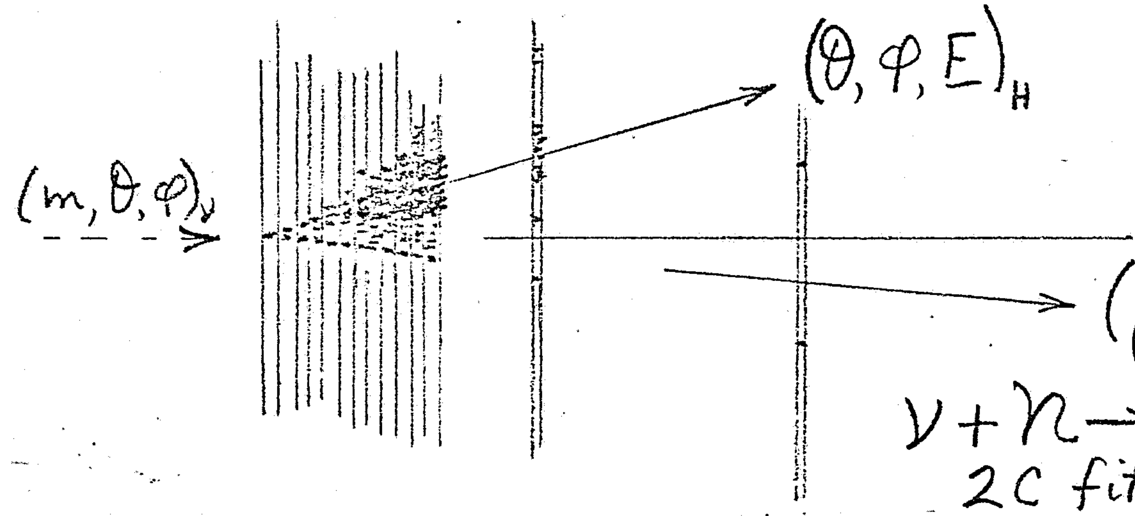

$\nu + n \rightarrow \mu^- + H$

2C fit with observed quantities shown

3C fit if p_H inferred from angular spread of hadrons

4C fit if also very narrow band

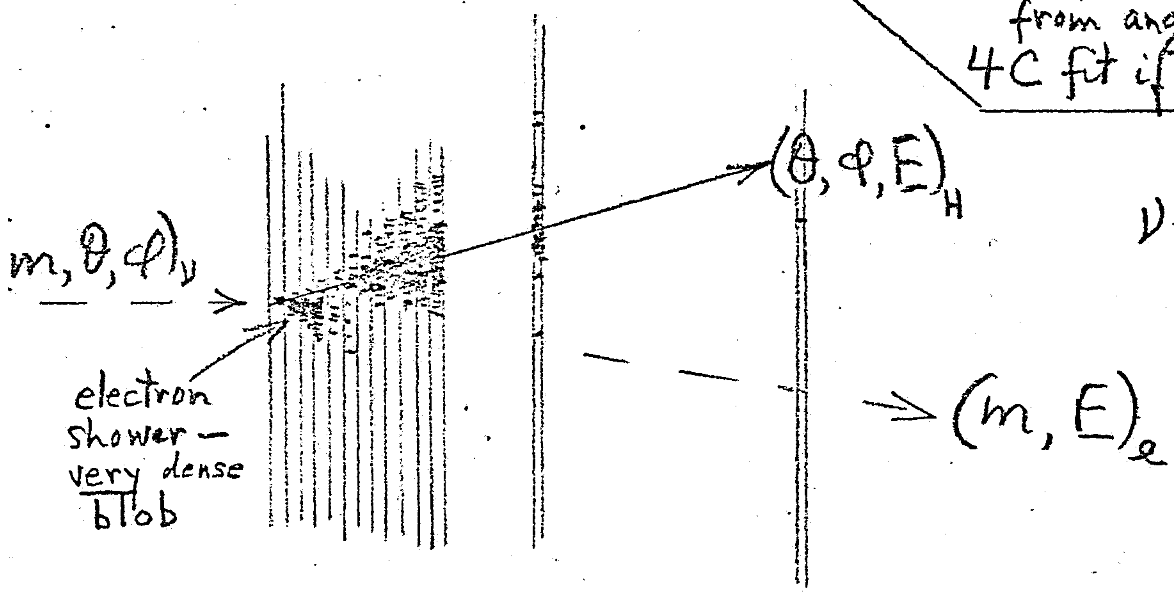

$\nu + n \rightarrow e^- + H$

0C as shown

1C if p_H inferred from $\langle \cos\theta_R \rangle$

2C if also E_ν know

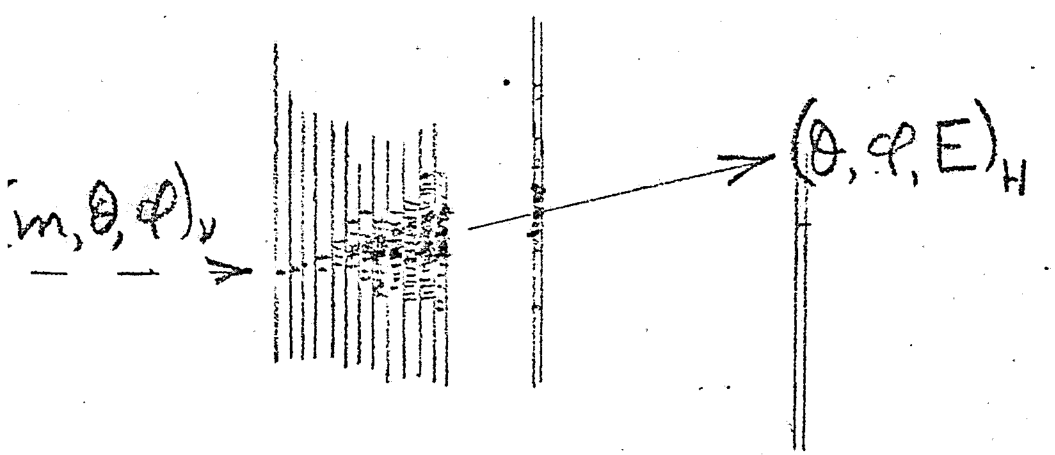

$\nu + n \rightarrow \nu + H$

−2C as shown

−1C if p_H from $\langle \cos\theta_h \rangle$

0C if also $m_\nu \equiv 0$ taken as missing ma